Relativistic Electrons Produced by Foreshock Disturbances Observed Upstream of Earth's Bow Shock

L. B. Wilson III* and D. G. Sibeck
NASA Goddard Space Flight Center, Greenbelt, Maryland 20771, USA

D. L. Turner
The Aerospace Corporation, El Segundo, California 90245, USA

A. Osmane
Department of Radio Science, Aalto University, Espoo 02150, Finland

D. Caprioli
Department of Astrophysical Sciences, Princeton University, Princeton, New Jersey 08544, USA and University of Chicago, Department of Astronomy and Astrophysics, Chicago, Illinois 60637, USA

V. Angelopoulos
Department of Earth, Planetary, and Space Sciences, and Institute of Geophysics and Planetary Physics, University of California, Los Angeles, Los Angeles, California 90095, USA

(Received 16 July 2016; published 14 November 2016)

Charged particles can be reflected and accelerated by strong (i.e., high Mach number) astrophysical collisionless shock waves, streaming away to form a foreshock region in communication with the shock. Foreshocks are primarily populated by suprathermal ions that can generate foreshock disturbances—large-scale (i.e., tens to thousands of thermal ion Larmor radii), transient (~5–10 per day) structures. They have recently been found to accelerate ions to energies of several keV. Although electrons in Saturn's high Mach number ($M > 40$) bow shock can be accelerated to relativistic energies (nearly 1000 keV), it has hitherto been thought impossible to accelerate electrons beyond a few tens of keV at Earth's low Mach number ($1 \leq M < 20$) bow shock. Here we report observations of electrons energized by foreshock disturbances to energies up to at least ~300 keV. Although such energetic electrons have been previously observed, their presence has been attributed to escaping magnetospheric particles or solar events. These relativistic electrons are not associated with any solar or magnetospheric activity. Further, due to their relatively small Larmor radii (compared to magnetic gradient scale lengths) and large thermal speeds (compared to shock speeds), no known shock acceleration mechanism can energize thermal electrons up to relativistic energies. The discovery of relativistic electrons associated with foreshock structures commonly generated in astrophysical shocks could provide a new paradigm for electron injections and acceleration in collisionless plasmas.

DOI: 10.1103/PhysRevLett.117.215101

Introduction.—Foreshock disturbances—large-scale (~1000 to > 30000 km), solitary [~5–10 per day, transient (lasting tens of seconds to several minutes)] structures [1,2]—generated by suprathermal (>100 eV to hundreds of keV) ions [3,4] arise upstream of Earth's bow shock formed by the solar wind colliding with Earth's magnetosphere. These disturbances have recently been found to accelerate ions to energies of several keV [5,6] and even produce their own foreshocks [7]. One type was found to have a distinct suprathermal electron population with energies >70 keV, which was attributed to a magnetospheric origin [8]. Although electrons in Saturn's high Mach number ($M > 40$) bow shock can be accelerated to relativistic energies (nearly 1000 keV) [9], it has hitherto been thought impossible to accelerate electrons at the much weaker ($M < 20$) Earth's bow shock beyond a few tens of keV [10]. Here we report observations of electrons energized by foreshock disturbances from tens of eV up to at least ~300 keV. We observe a single isotropic power law from hundreds of eV to hundreds of keV, unlike previous studies [8]. All previous observations of energetic foreshock electrons have been attributed to escaping magnetospheric particles [8,11,12] or solar events [13]. We observe no solar activity and the single isotropic power law cannot be explained by any magnetospheric source. Further, current theories of ion acceleration in foreshock disturbances cannot account for electrons accelerated to the observed relativistic energies [14–19].

Data sets.—We present observations from the THEMIS spacecraft [20] near foreshock disturbances. Quasistatic

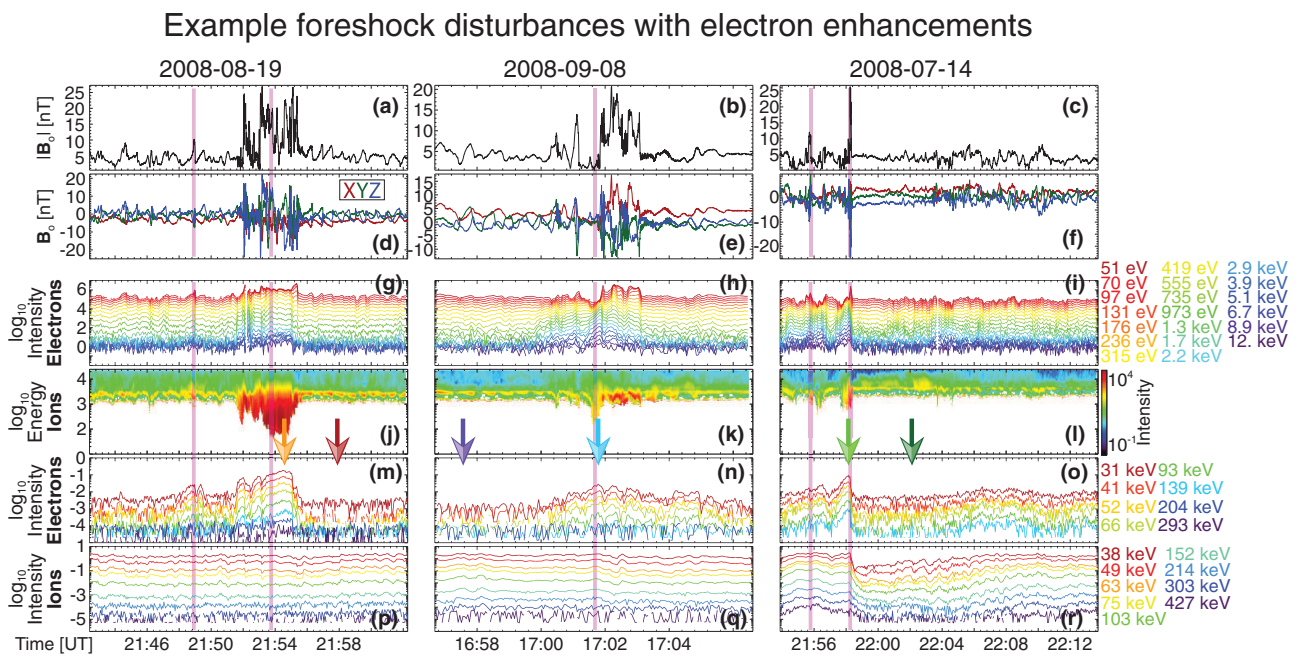

FIG. 1. Three example foreshock disturbances with energetic electron enhancements. All data were observed by THEMIS-C, with disturbance centers indicated by the vertical magenta lines. Magnetic fields are shown in units of nanotesla (nT) in the geocentric solar ecliptic coordinate basis. Particle data are shown in units of intensity ($cm^{-2}\ s^{-1}\ sr^{-1}\ eV^{-1}$) (or flux) as omnidirectional averages in the bulk flow rest frame with uniform color schemes (legends at far right) and vertical axis ranges by row. The low and high energy electron and high energy ion data are all shown as stacked line plots of intensity versus time, where each line corresponds to a different energy. The low energy ion data are shown as a dynamic energy spectrogram of energy versus time with a color scale [right-hand side of (l)] for intensity. (a)–(c) $|\mathbf{B}_0|$ (nT) at 4 samples per second. (d)–(f) $\mathbf{B}_0$ (nT) at 4 samples per second. (g)–(i) low energy electron (i.e., ~50 eV–12 keV) intensity. (j)–(l) Low energy ion (i.e., ~10 eV–25 keV) intensity. (m)–(o) High energy electron (i.e., ~30–300 keV) intensity. (p)–(r) High energy ion (i.e., ~30–430 keV) intensity.

(i.e., finite gain from zero up to Nyquist frequency) vector magnetic field measurements ($\mathbf{B}_0$) were obtained using the fluxgate magnetometer [21] at 4 and 128 samples per second. The data are presented in units of nanotesla (nT) in the geocentric solar ecliptic coordinate basis.

We examine in detail particle velocity distribution functions measured by the low energy (i.e., few eV to over 25 keV) electron and total ion electrostatic analyzers [22] and high energy (i.e., ~30 keV to over 500 keV) electron and total ion solid-state telescopes [23] with spin period (i.e., ~3 sec) resolution. All velocity distributions were transformed into the ion bulk flow reference frame by first converting to phase space density then performing a Lorentz transformation prior to any other unit conversions [24]. The azimuthal resolution is generally ~11.25° for the electrostatic analyzers and ~22.5° for the solid-state telescopes. The energy resolution is ~20% and ~30% for the electrostatic analyzers and solid-state telescopes, respectively.

Observations.—The disturbances occur in the ion foreshock [3,4] region upstream (sunward) of the quasiparallel bow shock, where the shock normal angle (θ_{Bn}) between the upstream quasistatic magnetic field ($\mathbf{B}_0$) and the shock normal vector satisfies $\theta_{Bn} < 45°$. We focused on observations near short large-amplitude magnetic structures [4], hot flow anomalies [1], and foreshock bubbles [2]. During the four orbital passes examined in detail, we identified 30 foreshock disturbances, ten of which had clear energetic electron enhancements (five at short large-amplitude magnetic structures, two at hot flow anomalies, and three at foreshock bubbles) [24].

We observe energetic (≥30 keV) electron enhancements as short duration (tens of seconds to a few minutes) enhancements in the electron fluxes above background by factors of ~10–200 (Fig. 1). When we examine the change in the ratio of the number density and energy flux of particles above ~200 eV to those below from outside the enhancements to those within, we find increases of factors of $\gtrsim$100 and $\gtrsim$50, respectively [24]. They are localized to the large fluctuations in $\mathbf{B}_0$ [Figs. 1(a)–1(c)] within the foreshock disturbances. The electron flux-time profiles for energies from ~0.25 to >200 keV show no energy dispersion; i.e., fluxes increase at all energies simultaneously [Figs. 1(g)–1(i) and 1(m)–1(o)]. The low energy electron [Figs. 1(g)–1(i)] and ion [Figs. 1(j)–1(l)] data look qualitatively similar for disturbances with and without [24] energetic electron enhancements. Note that nearly all disturbances show enhanced energetic ion fluxes often to >300 keV [Figs. 1(p)–1(r)]. The ion enhancements will be examined in future work.

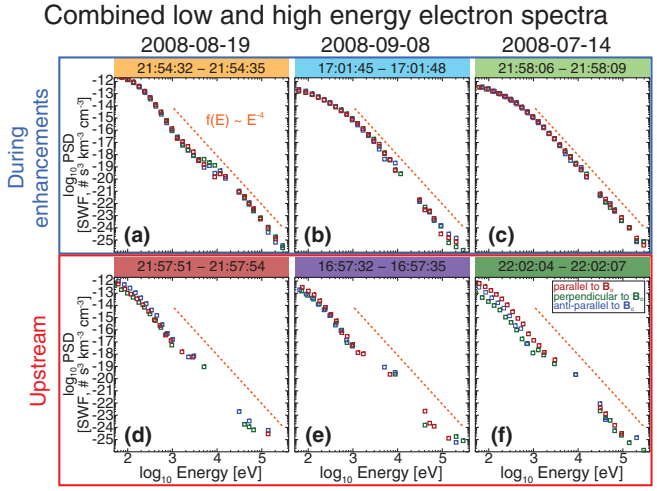

FIG. 2. Example pitch-angle spectra inside and outside electron enhancement periods for each of the example disturbances in Fig. 1. One-dimensional directional cuts (with respect to $\mathbf{B}_0$) of the merged particle velocity distributions from the low and high energy electron data, in units of phase space density ($s^{+3}\,cm^{-3}\,km^{-3}$), on log-log plots with uniform horizontal and vertical axis ranges of $\sim 10^{-26}$–10^{-12} $s^{+3}\,cm^{-3}\,km^{-3}$ and ~0.050–400 keV, respectively. The color-coded boxes above each plot correspond to the color-coded arrows in Fig. 1. Each panel shows cuts parallel (red), perpendicular (green), and antiparallel (blue) to $\mathbf{B}_0$, where missing data points indicate an absence of significant flux. The orange dashed line shows a power law [defined in (a)] for perspective. (a)–(c) Distributions during the peak energetic electron enhancements in Fig. 1. (d)–(f) Distributions during periods of inactivity in Fig. 1.

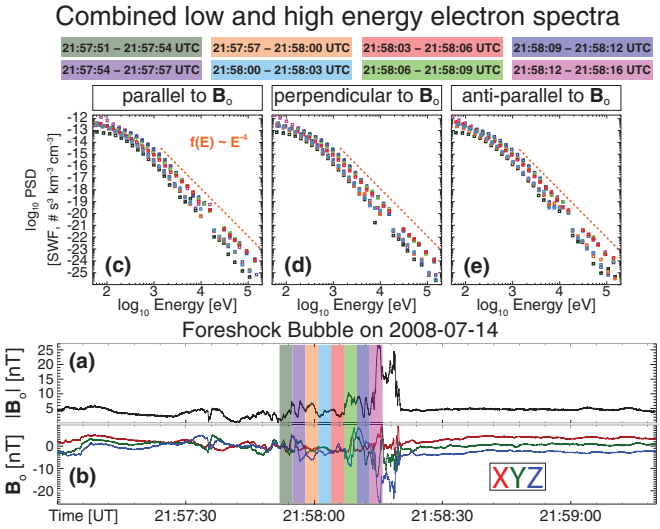

FIG. 3. Example time evolution of particle spectra in field-aligned coordinates during an enhancement within the foreshock bubble shown in Fig. 1 on 2008-07-14. Magnetic field data are in units of nanotesla (nT) in the geocentric solar ecliptic coordinate basis. Particle data are shown as one-dimensional cuts (similar to Fig. 2) in units of phase space density ($s^{+3}\,cm^{-3}\,km^{-3}$), on log-log plots with the same uniform horizontal and vertical axis ranges as in Fig. 2. The color-coded boxes above all particle distribution plots [(c)–(e)] correspond to the color-coded time ranges in the magnetic field plots below [(a) and (b)].

We then constructed pitch-angle—the angle between electron momentum and some reference vector, often $\mathbf{B}_0$—distributions from the particle data to compare distributions during energetic electron enhancements [Figs. 2(a)–2(c)] to those outside the enhancement periods [Figs. 2(d)–2(f)]. The electron distributions are observed to be almost isotropic from ~0.05 to 300 keV, with anisotropies (e.g., ratio of intensity or phase space density along $\mathbf{B}_0$ to that perpendicular to $\mathbf{B}_0$) rarely exceeding factors of 2. Note that the signal-to-noise ratio of the data above ~140 keV is near unity, and thus cannot be interpreted, for the 2008-09-08 hot flow anomaly [Fig. 2(b)] and 2008-07-14 foreshock bubble [Fig. 2(c)] example enhancements. The data also show a power-law form with $f(E) \propto E^{-4}$ from as low as ~0.25 keV up to highest energies observed during each enhancement [Figs. 2(a)–2(c)]. The distributions observed outside the enhancements [Figs. 2(d)–2(f)] show far more variability, only noise >12 keV, and in some cases significant anisotropies [Fig. 2(f)].

To illustrate the consistency of the single, isotropic power law, we present a time evolution of the distributions in field-aligned coordinates in Fig. 3. The three panels [i.e., Figs. 3(c)–3(e)] are split by orientation with respect to $\mathbf{B}_0$ but show a consistent, single, isotropic power law from hundreds of eV to $\gtrsim$140 keV for the eight distributions shown. The only significant variability is a change in phase space density from one distribution to the next.

Because of the high variability in $\mathbf{B}_0$ during the accumulation time of a single particle distribution, we also constructed pitch-angle distributions by sorting the pitch angles with subspin period time resolution, using algorithms similar to previous work [68], to remove artifacts of aliasing. We found that the isotropy was not a consequence of aliasing and is thus a real feature [24].

To verify that the enhancements were not of solar origin, we examined the *Wind* and twin STEREO spacecraft radio data for solar radio bursts, which were not observed during the energetic electron enhancements observed by THEMIS. We also examined the *Wind* particle data for energy-dispersed profiles characteristic of solar energetic electrons [13], which were also not observed. Finally, there were no interplanetary shocks, which can produce relativistic electrons [69,70], observed by *Wind* during any of the electron enhancements [24].

Next, we ruled out Earth's bow shock as a source by examining the following concepts. First, the two most viable shock acceleration mechanisms for electrons have the highest efficiencies in the quasiperpendicular ($\theta_{Bn} > 45°$) region of the shock [10,17]. Second, due to a higher mobility along versus across $\mathbf{B}_0$, any energetic electron distribution observed several Earth radii (i.e., tens to hundreds of Larmor

radii) away from the source would be highly anisotropic along $\mathbf{B}_0$, as previously reported [71], inconsistent with our observations [see, e.g., Figs. 2(a)–2(c)]. Third, the maximum observed energies are at most several tens of keV energies [69,70,72] seen as magnetic field-aligned beams at the electron foreshock edge, whereas we observe isotropic distributions up to at least ∼300 keV within the ion foreshock (Figs. 1 and 2). Finally, both of these mechanisms should produce some energy dispersion for observations far upstream of Earth's bow shock, which we do not observe (see, e.g., Figs. 1 and 3).

Another possibility is that the enhancements arise as a "pileup" of particles at the magnetic gradients, which act like mirrors. However, we do not observe energy-dispersed profiles within the magnetic compressions (i.e., due to energy-dependent Larmor radii effects and diffusion) or enhanced intensities outside the foreshock disturbances or pitch-angle distributions peaking perpendicular to $\mathbf{B}_0$. Further, the Larmor radius of a ∼90 keV electron, in the range of magnetic field magnitudes observed, span ∼26–1080 km. These values are comparable to and larger than the gradient scale length of most collisionless shock waves [4] and comparable to the scale size of some foreshock disturbances, which precludes adiabatic reflection between the two merging shocks [19]. Thus, we can rule out the "pileup" scenario as a source.

Previous reports of energetic electrons in the ion foreshock attributed the enhancements to a magnetospheric source [11,12,14]. One study [8] found energetic electrons (∼70–200 keV) within hot flow anomalies that were nearly isotropic, but they explicitly stated that the energetic electrons were a separate population from those at lower energies and that they were of magnetospheric origin. There are multiple differences between these results and our observations, including (1) while the magnetic compression regions of hot flow anomalies can be magnetically connected to the magnetosheath, the entire structure of the other two foreshock disturbances in our study can be isolated within the ion foreshock, (2) we observe a single, isotropic power law from hundreds of eV to ≥140 keV in many enhancements, indicative of a common acceleration mechanism (see, e.g., Figs. 2 and 3), and (3) the combination of a single power-law and an isotropic distribution over such a large range of energies cannot be explained by a magnetospheric source.

The enhancements were often observed with geomagnetic activity [11,12,14,73] and exhibited large anisotropies (ratios of sunward-to-antisunward fluxes [74] up to 5:1 and field-aligned-to-perpendicular fluxes [12] up to 6:1). Our observations are not consistent with any of these studies for the following reasons. First, since our electron distributions are nearly isotropic, they do not exhibit either highly field-aligned (Figs. 2 and 3) or antiearthward intensity anisotropies [24]. Second, we do not observe enhanced geomagnetic activity before or during any of the energetic electron enhancements [24].

Finally, the enhancements are always isolated within the foreshock disturbances, and thus are not consistent with escaping magnetospheric particles. The magnetic field direction variability is roughly the same within as without the disturbances. Thus, the probability of observing enhancements only within the disturbances (assuming the probability of occurrence is constant for all observations) is so negligibly small that by this alone we can rule out a nonlocal source [24].

Conclusions.—No previous work ever considered that foreshock disturbances could locally produce electrons to these energies. We estimated the maximum energy electrons could gain through shock drift acceleration [15,17,18], assuming highly idealized conditions for a foreshock bubble, to be at maximum ∼160–380 keV. More realistic estimates, but still ignoring curvature and fluctuating fields, are ∼56–133 keV. However, the same mechanism could only produce ∼3–6 keV electrons for short large-amplitude magnetic structures but we observe ≳300 keV electrons. We also made a preliminary examination for high-frequency waves finding both magnetosonic-whistler modes [4,68] and the higher-frequency whistler mode waves [75,76] in addition to several types of electrostatic waves at higher frequencies [76,77]. Yet when we compare the ratio of the fluctuating to quasistatic magnetic energy density for disturbances with and without energetic electron enhancements, we find no noticeable differences [24]. Future work will examine these modes in detail as a potential energization mechanism. Thus, it is not clear why only some disturbances produce enhancements, and current theory cannot explain the electron energization. Providing such an explanation is beyond the scope of this study.

The electron energization is not occurring locally at the main shock, but remotely within the ion foreshock. The most outstanding unanswered question in shock acceleration theory is the so-called "injection problem" (i.e., how to get thermal particles up to suprathermal energies before they are convected downstream), where previous work has only considered local energization at the shock. Therefore, these observations provide a new avenue through which electrons can be nonlocally preenergized to high enough energies to undergo further acceleration when interacting with astrophysical shocks. Given the ubiquity of foreshocks upstream of collisionless astrophysical shocks, we expect foreshock disturbances to be ubiquitous as well, which could fundamentally change our understanding of collisionless shocks.

The authors thank A. F.- Viñas, D. Bryant, V. Krasnoselskikh, M. Desai, B. Randol, J. Giacalone, F. Guo, A. W. Breneman, and E. R. Christian for useful discussions of the fundamental physics involved in our study. The authors thank J. R. Woodroffe and T. W. Kirkman for discussions of probabilities of rare events. The authors thank the CARISMA team (operated by the

University of Alberta and funded by the Canadian Space Agency), the *Wind* and STEREO teams, and NASA SPDF/CDAWeb for data. This work was funded by the Wind, MMS, THEMIS, and Van Allen Probes missions, the Aerospace Corp., NASA Grants No. NNX14AC16G and No. NNX16AQ50G, Grant No. N297688 from the Academy of Finland, and a NASA Heliophysics Supporting Research grant.

*lynn.b.wilsoniii@gmail.com

[1] N. Omidi and D. G. Sibeck, J. Geophys. Res. **112**, A1 (2007).
[2] D. L. Turner, N. Omidi, D. G. Sibeck, and V. Angelopoulos, J. Geophys. Res. **118**, 1552 (2013).
[3] D. Burgess, E. Möbius, and M. Scholer, Space Sci. Rev. **173**, 5 (2012).
[4] L. B. Wilson III, in *Low-Frequency Waves in Space Plasmas*, Geophysical Monograph Series Vol. 216, edited by A. Keiling, D.-H. Lee, and V. Nakariakov (American Geophysical Union, Washington, DC, 2016), pp. 269–291.
[5] A. Kis, O. Agapitov, V. Krasnoselskikh, Y. V. Khotyaintsev, I. Dandouras, I. Lemperger, and V. Wesztergom, Astrophys. J. **771**, 4 (2013).
[6] L. B. Wilson III, A. Koval, D. G. Sibeck, A. Szabo, C. A. Cattell, J. C. Kasper, B. A. Maruca, M. Pulupa, C. S. Salem, and M. Wilber, J. Geophys. Res. **118**, 957 (2013).
[7] T. Z. Liu, H. Hietala, V. Angelopoulos, and D. L. Turner, Geophys. Res. Lett. **43**, 4708 (2016).
[8] G. Paschmann, G. Haerendel, N. Sckopke, E. Moebius, and H. Luehr, J. Geophys. Res. **93**, 11279 (1988).
[9] A. Masters, L. Stawarz, M. Fujimoto, S. J. Schwartz, N. Sergis, M. F. Thomsen, A. Retinò, H. Hasegawa, B. Zieger, G. R. Lewis, A. J. Coates, P. Canu, and M. K. Dougherty, Nat. Phys. **9**, 164 (2013).
[10] C. S. Wu, J. Geophys. Res. **89**, 8857 (1984).
[11] S. M. Krimigis, D. Venkatesan, J. C. Barichello, and E. T. Sarris, Geophys. Res. Lett. **5**, 961 (1978).
[12] E. T. Sarris, G. C. Anagnostopoulos, and S. M. Krimigis, J. Geophys. Res. **92**, 12083 (1987).
[13] R. E. Ergun, D. Larson, R. P. Lin, J. P. McFadden, C. W. Carlson, K. A. Anderson, L. Muschietti, M. McCarthy, G. K. Parks, H. Reme, J. M. Bosqued, C. D'Uston, T. R. Sanderson, K. P. Wenzel, M. Kaiser, R. P. Lepping, S. D. Bale, P. Kellogg, and J.-L. Bougeret, Astrophys. J. **503**, 435 (1998).
[14] G. C. Anagnostopoulos, A. G. Rigas, E. T. Sarris, and S. M. Krimigis, J. Geophys. Res. **103**, 9521 (1998).
[15] D. Caprioli and A. Spitkovsky, Astrophys. J. **783**, 91 (2014).
[16] M. A. Malkov and L. O. Drury, Rep. Prog. Phys. **64**, 429 (2001).
[17] J. Park, C. Ren, J. C. Workman, and E. G. Blackman, Astrophys. J. **765**, 147 (2013).
[18] J. Park, D. Caprioli, and A. Spitkovsky, Phys. Rev. Lett. **114**, 085003 (2015).
[19] R. A. Treumann, Astron. Astrophys. Rev. **17**, 409 (2009).
[20] V. Angelopoulos, Space Sci. Rev. **141**, 5 (2008).
[21] H. U. Auster *et al.*, Space Sci. Rev. **141**, 235 (2008).
[22] J. P. McFadden, C. W. Carlson, D. Larson, M. Ludlam, R. Abiad, B. Elliott, P. Turin, M. Marckwordt, and V. Angelopoulos, Space Sci. Rev. **141**, 277 (2008).
[23] B. Ni, Y. Shprits, M. Hartinger, V. Angelopoulos, X. Gu, and D. Larson, J. Geophys. Res. **116**, A03208 (2011).
[24] See Supplemental Material at http://link.aps.org/supplemental/10.1103/PhysRevLett.117.215101, which includes Refs. [25–67], for more details about the coordinate systems, reference frames, calculation of data quantities, spacecraft orbits, examples of disturbances without electron enhancements, radio observations, additional pitch-angle distribution examples, elimination of the magnetospheric source showing no geomagnetic activity, elimination of solar source, discussion of high-frequency wave mode observations, quantitative estimates of density and energy flux of the enhancements, shock drift acceleration discussion, and probability of occurrence estimates.
[25] D. Burgess and M. Scholer, Space Sci. Rev. **178**, 513 (2013).
[26] J. A. Slavin and R. E. Holzer, J. Geophys. Res. **86**, 11401 (1981).
[27] M. A. Riquelme and A. Spitkovsky, Astrophys. J. **733**, 63 (2011).
[28] M. Oka, T. Terasawa, Y. Seki, M. Fujimoto, Y. Kasaba, H. Kojima, I. Shinohara, H. Matsui, H. Matsumoto, Y. Saito, and T. Mukai, Geophys. Res. Lett. **33**, L24104 (2006).
[29] E. A. Lucek, T. S. Horbury, I. Dandouras, and H. Rème, J. Geophys. Res. **113**, n/a (2008).
[30] G. Mann, H. Luehr, and W. Baumjohann, J. Geophys. Res. **99**, 13315 (1994).
[31] M. Scholer, H. Kucharek, and I. Shinohara, J. Geophys. Res. **108**, 1273 (2003).
[32] S. J. Schwartz, D. Burgess, W. P. Wilkinson, R. L. Kessel, M. Dunlop, and H. Luehr, J. Geophys. Res. **97**, 4209 (1992).
[33] J. P. Eastwood, D. G. Sibeck, V. Angelopoulos, T. D. Phan, S. D. Bale, J. P. McFadden, C. M. Cully, S. B. Mende, D. Larson, S. Frey, C. W. Carlson, K.-H. Glassmeier, H. U. Auster, A. Roux, and O. Le Contel, Geophys. Res. Lett. **35**, L17S03 (2008).
[34] N. Omidi, H. Zhang, D. Sibeck, and D. Turner, J. Geophys. Res. **118**, 173 (2013).
[35] N. Omidi, H. Zhang, C. Chu, D. Sibeck, and D. Turner, J. Geophys. Res. **119**, 9823 (2014).
[36] S. J. Schwartz, C. P. Chaloner, D. S. Hall, P. J. Christiansen, and A. D. Johnstones, Nature (London) **318**, 269 (1985).
[37] H. Zhang, D. G. Sibeck, Q.-G. Zong, S. P. Gary, J. P. McFadden, D. Larson, K.-H. Glassmeier, and V. Angelopoulos, J. Geophys. Res. **115**, A12235 (2010).
[38] H. Zhang, D. G. Sibeck, Q.-G. Zong, N. Omidi, D. Turner, and L. B. N. Clausen, J. Geophys. Res. **118**, 3357 (2013).
[39] M. O. Archer, D. L. Turner, J. P. Eastwood, S. J. Schwartz, and T. S. Horbury, Planet. Space Sci. **106**, 56 (2015).
[40] N. Omidi, J. P. Eastwood, and D. G. Sibeck, J. Geophys. Res. **115**, A06204 (2010).
[41] T. Z. Liu, D. L. Turner, V. Angelopoulos, and N. Omidi, J. Geophys. Res. **121**, 5489 (2016).
[42] J.-L. Bougeret, M. L. Kaiser, P. J. Kellogg, R. Manning, K. Goetz, S. J. Monson, N. Monge, L. Friel, C. A. Meetre, C. Perche, L. Sitruk, and S. Hoang, Space Sci. Rev. **71**, 231 (1995).

[43] J. L. Bougeret *et al.*, Space Sci. Rev. **136**, 487 (2008).
[44] R. E. Ergun, C. W. Carlson, J. P. McFadden, F. S. Mozer, G. T. Delory, W. Peria, C. C. Chaston, M. Temerin, R. Elphic, R. Strangeway, R. Pfaff, C. A. Cattell, D. Klumpar, E. Shelly, W. Peterson, E. Moebius, and L. Kistler, Geophys. Res. Lett. **25**, 2061 (1998).
[45] R. P. Lin, K. A. Anderson, S. Ashford, C. Carlson, D. Curtis, R. Ergun, D. Larson, J. McFadden, M. McCarthy, G. K. Parks, H. Rème, J. M. Bosqued, J. Coutelier, F. Cotin, C. D'Uston, K.-P. Wenzel, T. R. Sanderson, J. Henrion, J. C. Ronnet, and G. Paschmann, Space Sci. Rev. **71**, 125 (1995).
[46] M. M. Leroy and A. Mangeney, Ann. Geophys. **2**, 449 (1984).
[47] Y. Hobara, M. Balikhin, V. Krasnoselskikh, M. Gedalin, and H. Yamagishi, J. Geophys. Res. **115**, n/a (2010).
[48] C. Mazelle, B. Lembège, A. Morgenthaler, K. Meziane, T. S. Horbury, V. Génot, E. A. Lucek, and I. Dandouras, in *Proceedings of the Twelfth International Solar Wind Conference* (AIP, Saint-Malo, 2010), Vol. 1216, p. 471.
[49] G. C. Anagnostopoulos and G. D. Kaliabetsos, J. Geophys. Res. **99**, 2335 (1994).
[50] G. C. Anagnostopoulos, V. Tenentes, and E. S. Vassiliadis, J. Geophys. Res. **114**, n/a (2009).
[51] X. Guo, L. Sironi, and R. Narayan, Astrophys. J. **797**, 47 (2014).
[52] L. Ball and D. B. Melrose, Pub. Astron. Soc. Aust. **18**, 361 (2001).
[53] K. A. Anderson, J. Geophys. Res. **86**, 4445 (1981).
[54] P. Savoini, B. Lembége, and J. Stienlet, J. Geophys. Res. **115**, A09104 (2010).
[55] E. T. Sarris, S. M. Krimigis, and T. P. Armstrong, J. Geophys. Res. **81**, 2341 (1976).
[56] I. R. Mann, D. K. Milling, I. J. Rae, L. G. Ozeke, A. Kale, Z. C. Kale, K. R. Murphy, A. Parent, M. Usanova, D. M. Pahud, E.-A. Lee, V. Amalraj, D. D. Wallis, V. Angelopoulos, K.-H. Glassmeier, C. T. Russell, H.-U. Auster, and H. J. Singer, Space Sci. Rev. **141**, 413 (2008).
[57] J. P. McFadden, C. W. Carlson, D. Larson, J. Bonnell, F. Mozer, V. Angelopoulos, K.-H. Glassmeier, and U. Auster, Space Sci. Rev. **141**, 477 (2008).
[58] D. L. Turner, V. Angelopoulos, W. Li, M. D. Hartinger, M. Usanova, I. R. Mann, J. Bortnik, and Y. Shprits, J. Geophys. Res. **118**, 2196 (2013).
[59] F. Bordoni, Nucl. Instrum. Methods **97**, 405 (1971).
[60] R. R. Goruganthu and W. G. Wilson, Rev. Sci. Instrum. **55**, 2030 (1984).
[61] C. Meeks and P. B. Siegel, Am. J. Phys. **76**, 589 (2008).
[62] J. A. Schecker, M. M. Schauer, K. Holzscheiter, and M. H. Holzscheiter, Nucl. Instrum. Methods Phys. Res., Sect. A **320**, 556 (1992).
[63] D. W. Curtis, C. W. Carlson, R. P. Lin, G. Paschmann, and H. Reme, Rev. Sci. Instrum. **60**, 372 (1989).
[64] G. Paschmann and P. W. Daly, ISSI Sci. Rep. Ser. **1** (1998).
[65] Calibration of Particle Instruments in Space Physics, edited by M. Wüest, D. S. Evans, and R. von Steiger (ESA Publications Division, Noordwijk, Netherlands, 2007).
[66] A. H. Compton and I. A. Getting, Phys. Rev. **47**, 817 (1935).
[67] F. M. Ipavich, Geophys. Res. Lett. **1**, 149 (1974).
[68] L. B. Wilson III, A. Koval, A. Szabo, A. Breneman, C. A. Cattell, K. Goetz, P. J. Kellogg, K. Kersten, J. C. Kasper, B. A. Maruca, and M. Pulupa, Geophys. Res. Lett. **39**, L08109 (2012).
[69] M. I. Desai and D. Burgess, J. Geophys. Res. **113**, A00B06 (2008).
[70] E. T. Sarris and S. M. Krimigis, Astrophys. J. **298**, 676 (1985).
[71] K. A. Anderson, R. P. Lin, F. Martel, C. S. Lin, G. K. Parks, and H. Reme, Geophys. Res. Lett. **6**, 401 (1979).
[72] J. T. Gosling, M. F. Thomsen, S. J. Bame, and C. T. Russell, J. Geophys. Res. **94**, 10011 (1989).
[73] E. A. Kronberg, R. Bučík, S. Haaland, B. Klecker, K. Keika, M. I. Desai, P. W. Daly, M. Yamauchi, R. Gómez-Herrero, and A. T. Y. Lui, J. Geophys. Res. **116**, n/a (2011).
[74] G. C. Anagnostopoulos, E. T. Sarris, and S. M. Krimigis, J. Geophys. Res. **91**, 3020 (1986).
[75] L. B. Wilson III, A. Koval, A. Szabo, A. Breneman, C. A. Cattell, K. Goetz, P. J. Kellogg, K. Kersten, J. C. Kasper, B. A. Maruca, and M. Pulupa, J. Geophys. Res. **118**, 5 (2013).
[76] L. B. Wilson III, D. G. Sibeck, A. W. Breneman, O. Le Contel, C. Cully, D. L. Turner, V. Angelopoulos, and D. M. Malaspina, J. Geophys. Res. **119**, 6475 (2014).
[77] L. B. Wilson III, D. G. Sibeck, A. W. Breneman, O. Le Contel, C. Cully, D. L. Turner, V. Angelopoulos, and D. M. Malaspina, J. Geophys. Res. **119**, 6455 (2014).